Modeling of *in situ* Heat Treatment in Austempered Ductile Iron

S.-M. Yoo, A. Ludwig, K. Moeinipour and P. R. Sahm

Gießerei-Institut der RWTH-Aachen
D-52056 Aachen, Germany

ABSTRACT

The material properties of cast irons depend mainly on the structure of the matrix in as-cast condition or after of heat treatment. A simulation model has been developed to predict the microstructural evolution during solidification of spheroidal graphite (SG) cast iron in gravity die casting and the subsequent solid state transformations during *in situ* heat treatment. The fraction of solid, the nodule sizes, the nodule counts and the fraction of solid state phases which form during austempering were calculated in this model. The temperature distribution during the solidification in a permanent mould and during the subsequent austempering heat treatment was determined. The bainitic transformation occurring during the austempering was simulated by the Avrami equation. The simulation was verified with experimental results.

1. INTRODUCTION

The mechanical properties of the casting alloys depend mainly on the structure of the matrix in the as-cast condition or after heat treatment. In spheroidal graphite cast iron and austempered ductile iron (ADI) the nodularity of the graphite phase is also very important for the material characteristics. If the microstructural evolution and the phase transformation of the nodular cast iron can be determined by numerical simulation, the mechanical properties of the final material can be predicted.

After the early work of Oldfield [1] and Wetterfall *et al.* [2], much work has been carried out on the modelling of the solidification and solid state transformation of nodular cast iron [3, 4]. Recently the microsegregation of silicon during solidification has been taken into account [5, 6]. The solidification of nodular cast iron can be calculated by nucleation and growth of grains in terms of carbon diffusion through austenite shells [2-6]. The formation rate of ferrite can be predicted on the assumption that it is controlled by the diffusion rate of carbon through the ferrite shell under steady state [4, 5, 7]. The fraction of pearlite formed and the evolution of bainite during austempered heat treatment can be calculated by the Avrami equation [8-11].

The object of this work is to simulate the microstructural evolution of nodular cast iron during the solidification and subsequent *in situ* heat treatment.

2. COMPUTATIONAL MODEL

When the melt temperature falls below the eutectic temperature, eutectic grains are formed. In the present model the nucleation rate is assumed to be presented in terms of undercooling by a power law function [3]. It is assumed that these grains consist of graphite spheres enveloped by an austenite shell (Fig. 1) and that their growth is controlled by carbon diffusion [2, 3]. The growth rate of the austenite shell and the graphite nodule under quasi-steady state conditions can be obtained from carbon mass balances at each boundary [3]. The eutectic and eutectoid temperature which depend on the amount of silicon in the alloy as well as the carbon concentrations at any interfaces are obtained from thermodynamic phase

equilibrium calculations performed with the commercial software tool ChemApp, the FORTRAN library of ChemSage [12].

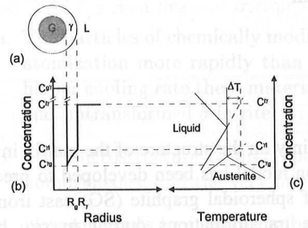

Fig. 1 Schematic eutectic growth model (a), distribution of carbon concentration (b) and schematic quasi-equilibrium phase diagram (c).

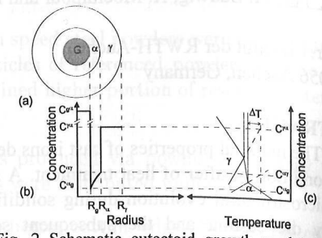

Fig. 2 Schematic eutectoid growth model (a), distribution of carbon concentration (b) and schematic quasi-equilibrium phase diagram (c).

If there is no decomposition of pearlite to ferrite and graphite and assuming that (i) the growth of the ferrite shell into the austenite is controlled by carbon diffusion in quasi-steady state and (ii) the concentration gradient in the austenite has already disappeared, the growth rate of the ferrite shell and nodular graphite can be calculated from mass conservation [4, 5, 7] (Fig. 2).

The transformation from austenite to pearlite or bainite is described by the Avrami equation [8]. The Avrami coefficients, *c(T)* and *n(T)*, have been determined at each temperature from the "start" and "end" of isotransformation curves on the TTT-diagram taken from ref. [13]. To calculate the amount of phase change during continuous cooling the Avrami equation was solved by applying the additivity rule to the fractions transformed using the isothermal transformation data, *c(T)* and *n(T)* [9-11].

3. EXPERIMENTAL PROCEDURE

The casting and the permanent mould system used in this work is shown in Fig. 3. Dimensions are given in mm. The casting and mould were enmeshed with 115736 volume elements. The enmeshment of the casting is illustrated in Fig. 4.

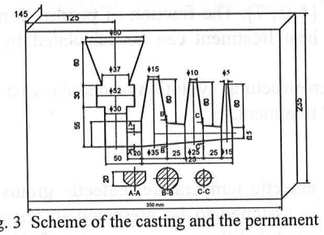

Fig. 3 Scheme of the casting and the permanent mould system.

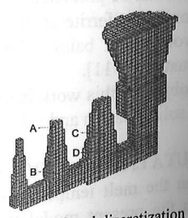

Fig. 4 Three-dimensional discretization of one half of the cast part as used for the calculation.

A charge composed of pig iron, steel and ferro-silicon was melted in a middle-frequency induction furnace. It was treated with 0.5 kg FeSiMg10 alloy for spheroidization and K40 Germalloy for inoculation. After treatment the melt was poured into a permanent mould. The pouring temperature was 1410°C. The cast iron permanent mould was pre-heated to 280°C. To reduce the heat flow between the mould and the casting, a special coating system with insulation and metallurgical coating were used. The chemical composition of the nodular cast iron used in this work is listed in Table 1. The permanent mould was opened 20 seconds after mould filling and the casting was austempered in a salt bath at 375°C for 30 minutes.

Table 1 Chemical composition of nodular cast iron

Fe	C	Si	Mn	P	S	Cr	Mo	Ni	Cu	Mg
Bal.	3.59	3.52	0.0533	0.020	0.0079	0.0371	0.305	0.06	0.0239	0.0292

4. RESULTS AND DISCUSSION

Fig. 5-6 showed a typical microstructure at the centre and near the surface of the casting. The influence of the cooling conditions is obvious. As expected, the nodule sizes at the surface were smaller than that at the centre. Fig. 7 shows the calculated cooling curves and the variations of the solid fraction at different positions. The cooling rate in the vicinity of the surface of the casting was very high, so that the nodule counts at this location are highly affected. As the temperature at that position was already below A_{C1} before the quenching process began no transformation into bainite was observed (Fig. 7).

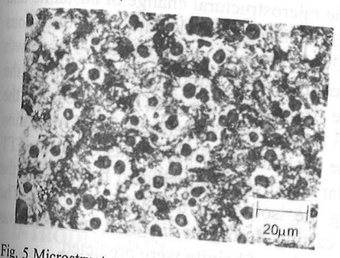

Fig. 5 Microstructure of nodular cast iron near the surface of the casting (position A).

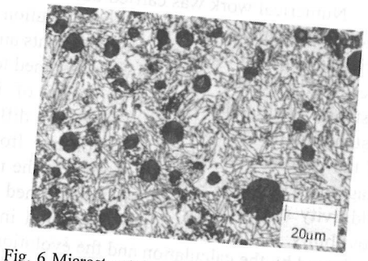

Fig. 6 Microstructure of nodular cast iron at the centre of the casting (position B).

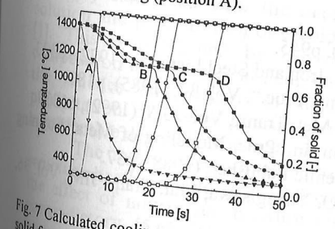

Fig. 7 Calculated cooling curves and evolutions of solid fraction at different positions in the casting.

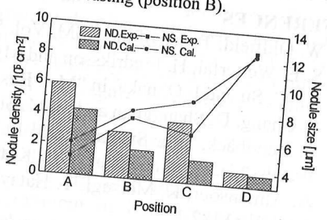

Fig. 8 Comparison of experimentally determined nodule counts and nodule sizes with calculation at different positions.

Nodule count is one of the most important parameters in nodular cast iron. The calculated and experimentally measured mean nodule counts at different locations of the casting and the corresponding nodule sizes are shown in Fig. 8. The calculated nodule counts and nodule sizes agree well with the experimental results.

The calculated evolution of the bainite is shown in Fig. 9. Like the experimental

findings, the calculation predicts that the matrix at the surface of casting (position A) is not transformed into bainite. In the bulk of the casting the austenite matrix is almost fully transformed into bainite (Fig. 6). This is also predicted by the calculation (Fig. 9). Finally the mechanical properties of the casting are listed in Table 2.

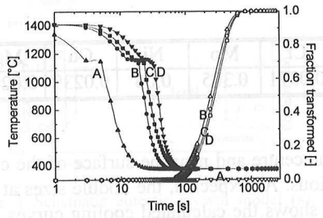

Fig. 9 Evolution of bainite in the casting at different positions.

Table 2 Mechanical properties of the casting.

Tensile strength	(N/mm^2)	889
Yield strength	(N/mm^2)	577
Elongation	(%)	7.22

5. CONCLUSIONS

Numerical work was carried out to simulate the microstructural change of austenite and spheroidal graphite during the solidification process and the solid state transformations during *in situ* heat treatment. Nodule counts and nodule sizes were also predicted. The growth rates of graphite and austenite were assumed to be controlled by carbon diffusion through the austenite shell. The rate of evolution of ferrite from austenite was evaluated on the assumption that it is controlled by carbon diffusion through the ferrite shell. The formulation of the pearlite and bainite evolution rate from the austenite matrix was based on the TTT diagram. The bainitic transformation in the nodular cast iron was predicted by applying the additivity rule to the fractions transformed using the isothermal transformation data. The possibility of the bainitic transformation in the casting during *in situ* heat treatment was evaluated by the calculation and the evolutions of fraction of bainite were predicted.

REFERENCES

1. W. Oldfield, Trans. of the ASM, Vol. 59, (1966), p945.
2. S. E. Wetterfal, H. Fredriksson and M. Hillert, J. Iron and Steel Institute, (1972), p323.
3. K. -C. Su and I. Ohnaka, in "Mat. Res. Soc. Symp. Proc.", Vol. 34, (1985), p181.
4. S. Chang, D. Shangguan and D. M. Stefanescu, Met. Trans., Vol. 23A, (1992), p1333.
5. E. Lundbäck, I. L. Svensson and P. E. Persson, in "Proc. Modeling of Metal Forming Process", eds. J. L. Chenot *et al*., Kluwer Academic Publisher, (1988), p37.
6. A. Almansour, K. Matsugi, T. Hatayama and O. Yanagisawa, Mat. Trans. JIM, Vol. 36, (1995), p1487.
7. D. Venugopalan, Met. Trans., Vol. 21A, (1990), p913.
8. M. Avrami, J. Chem. Phy., Vol. 7, (1939), p1103 and Vol. 4, (1940), p212.
9. E. Scheil, Arch. Eisenhüttenwes., Vol. 12, (1935), p565.
10. I. Tzitzelkov, H. P. Hougardy and A. Rose, Arch. Eisenhüttenwes., Nr. 8, (1974), p525.
11. F. M. B. Fernandes, S. Denis and A. Simon, Mat. Sci. And Tech., Vol. 1, (1985), p838.
12. G. Eriksson and K. Hack, Met. Trans., Vol. 21B, (1990), p1030.
13. K. Röhrig and W. Fairhurst, "Heat Treatment of Nodular Cast Iron", Giesserei-Verlag GmbH, (1979).